Improved highly efficient Dion-Jacobson type perovskite light-emitting diodes by effective surface polarization architecture

Supporting Information

Hanjun Yang [a, b], Jun Tang[a], Liangliang Deng [a], Zhe Liu [a], Xia Yang [c], Zengqi Huang [d], Haomiao Yu [a], Kai Wang [a] and Jinpeng Li [a] *

[a]Key Laboratory of Luminescence and Optical Information, Ministry of Education, School of Science, Beijing Jiaotong University, Beijing 100044, China

[b]Jiangxi Key Laboratory of Flexible Electronics, Flexible Electronics Innovation Institute, Jiangxi Science & Technology Normal University, Nanchang 330013, Jiangxi, China

[c]Department of Materials Science and Engineering, University of Science and Technology Beijing, Beijing 100083, China.

[d]Key Laboratory of Green Printing, Institute of Chemistry, Chinese Academy of Sciences (ICCAS), 2 Zhongguancun Beiyi Street, Beijing 100190, China

Table S1. Summarized performance of DJ type perovskite light-emitting diodes reported in previous and present works.

The device structure	Type of pervosite	Color	EL spectrum and parameters	Ref.
ITO/PEDOT:PSS/ $PEA_2MA_2Pb_3I_{10}$ (with MACl)/PCBM/PEI/Ag	Quasi-2D	8.64%	EL:645 nm EQE_{max}=2.2% L_{max}=1598 cd/m^2	Our work
ITO/PEDOT:PSS/$MAPbBrI_2$/P C_{61}BM/Ca/Al	3D	14.02%	EL:690 nm L_{max}=1710 cd/m^2	[1]
ITO/SnO_2/$MAPbI_3$/Spiro-OMeTAD (FN-Br)/Au	3D	21.54%	EL:772 nm EQE_{max}=4.3%	[2]
FTO/TiO_2/2D|3D heterostructure /Spiro-OMeTAD/Au	2D|3D heterostructure	21.02%	EL:771 nm EQE_{max}=5.13%	[3]
ITO/PEDOT:PSS/$MAPbBr_2I$/P CBM/ LiF/Al	3D	5-8%	EL:690-750 nm EQE_{max}=0.03%	[4]
FTO/NiO/$MAPbI_3$-QDs /PCBM/Ag	Quantum dot	17.1%	EL:778 nm EQE_{max}=0.084%	[5]
ITO/PEDOT:PSS/$MAPbBr_3$/Zn O/ $PEIBIm_4$/Ag	3D	2.41%	EL:778 nm EQE_{max}=0.0011% L_{max}=9 cd/m^2	[6]

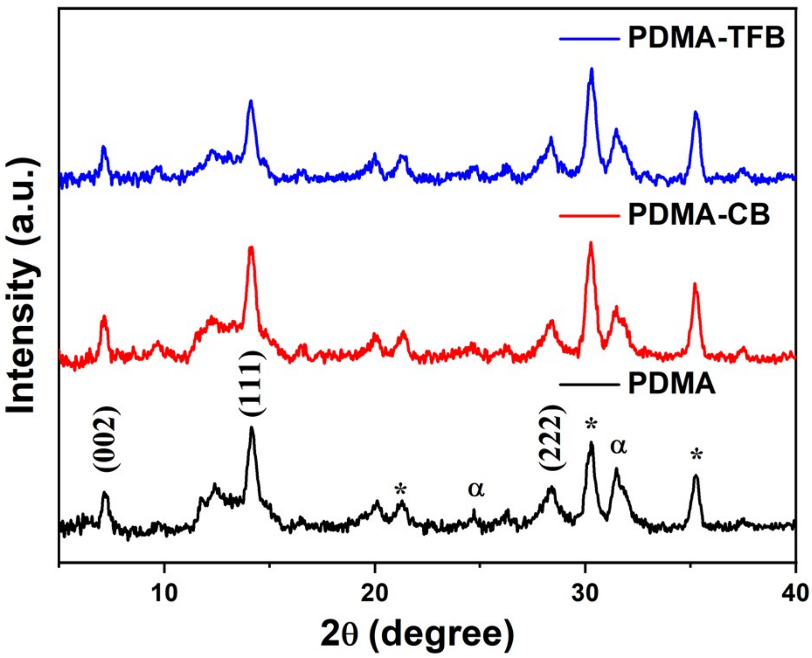

Figure S1. XRD patterns of perovskite films by different treatment upon ITO/ZnO/PEIE. * and α markers represent ITO and $FAPbI_3$.

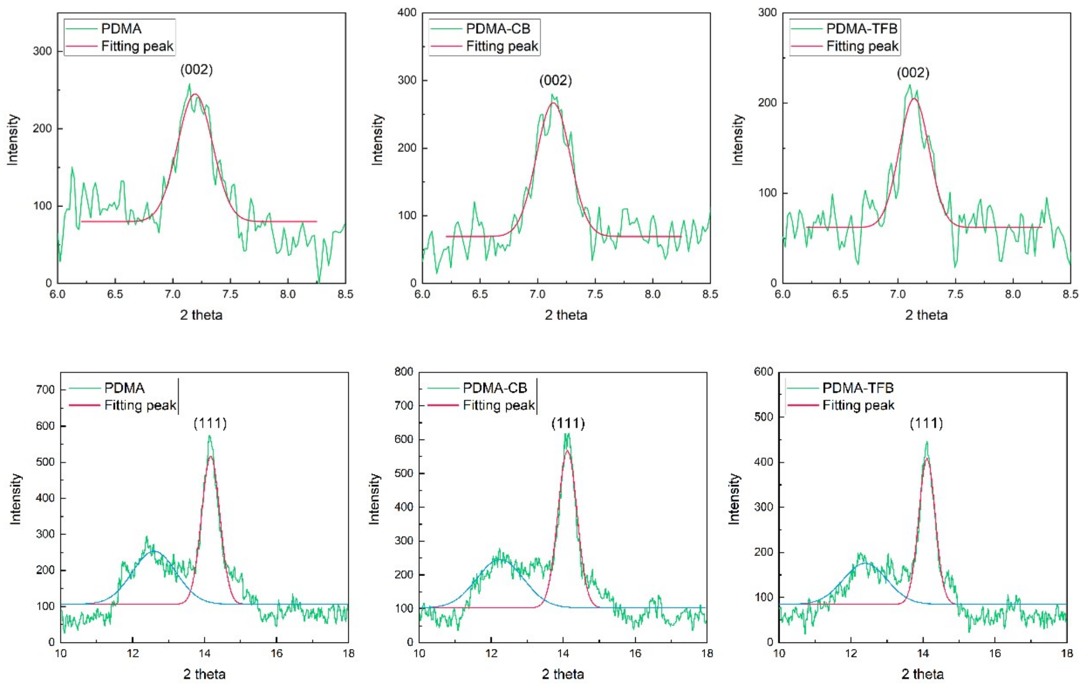

Figure S2. XRD pattern of (002) and (111) planes and their fitting results of all samples.

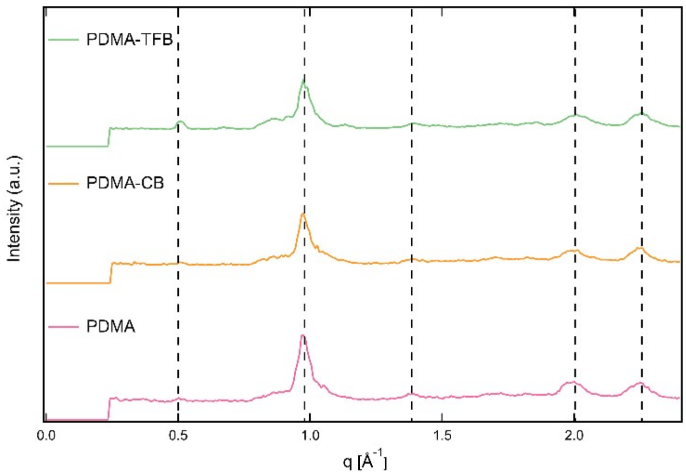

Figure S3. Radical integrated intensity of reciprocal space maps for three samples.

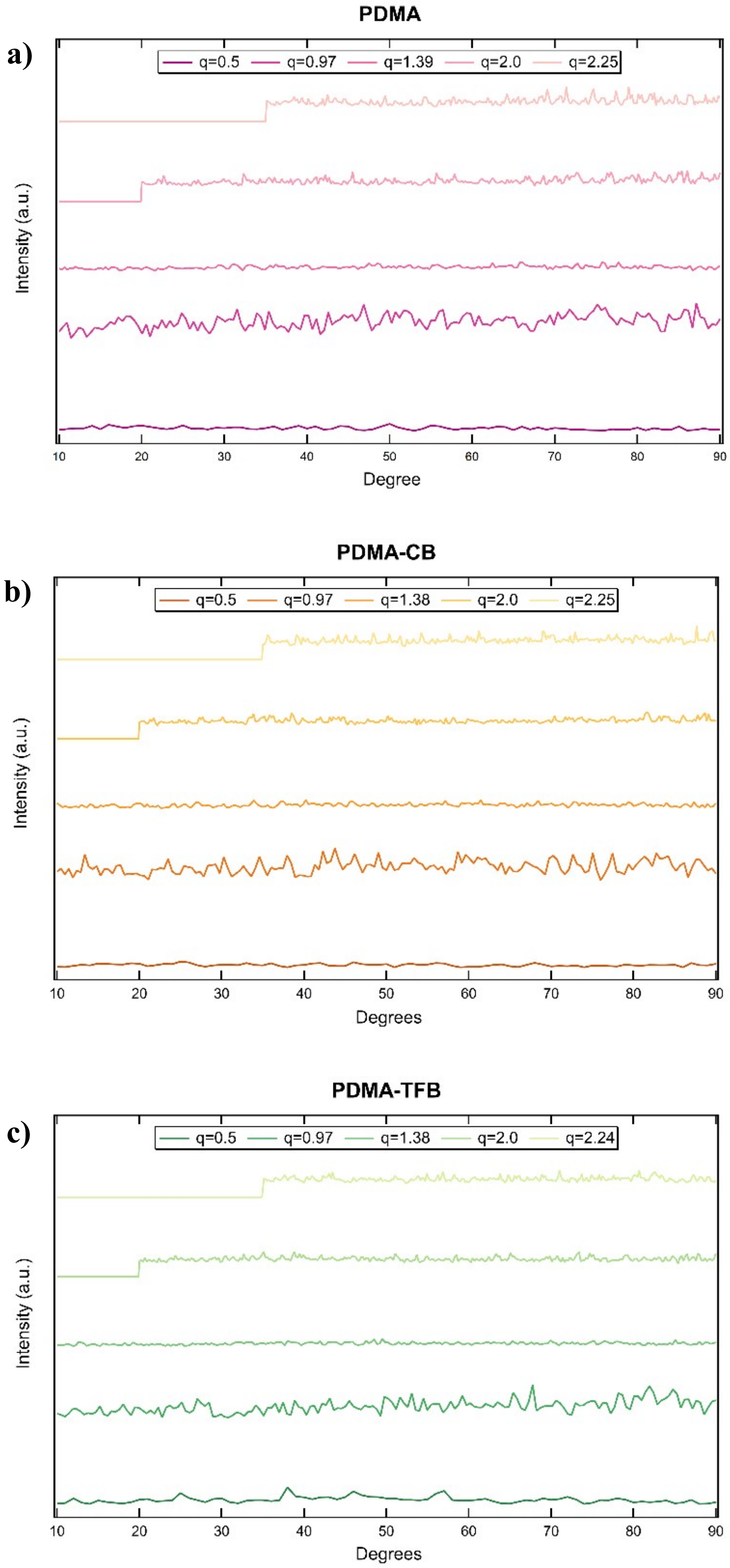

Figure S4. The azimuthal distribution intensity extracted from q-maps for three samples a) PDMA, b) PDMA-CB, c) PDMA-TFB.

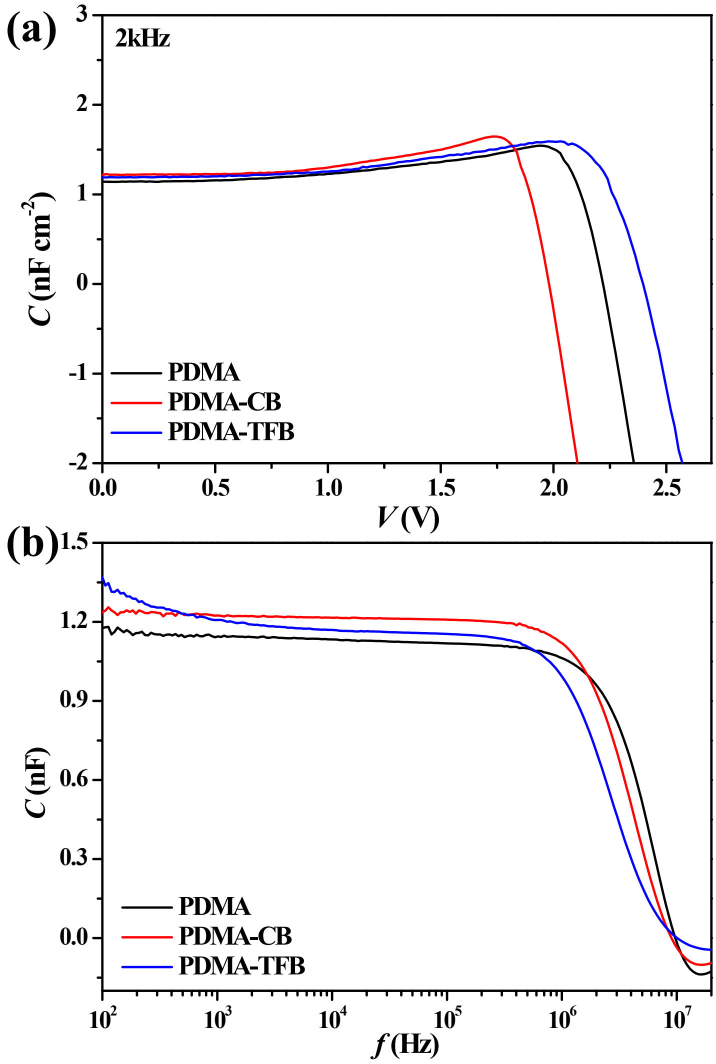

Figure S5. (a) Capacitance as a function of voltage (C-V) (b) Room temperature *C-f* spectra for DJ-PLEDs with different treatment for frequencies of 2kHz in dark condition.

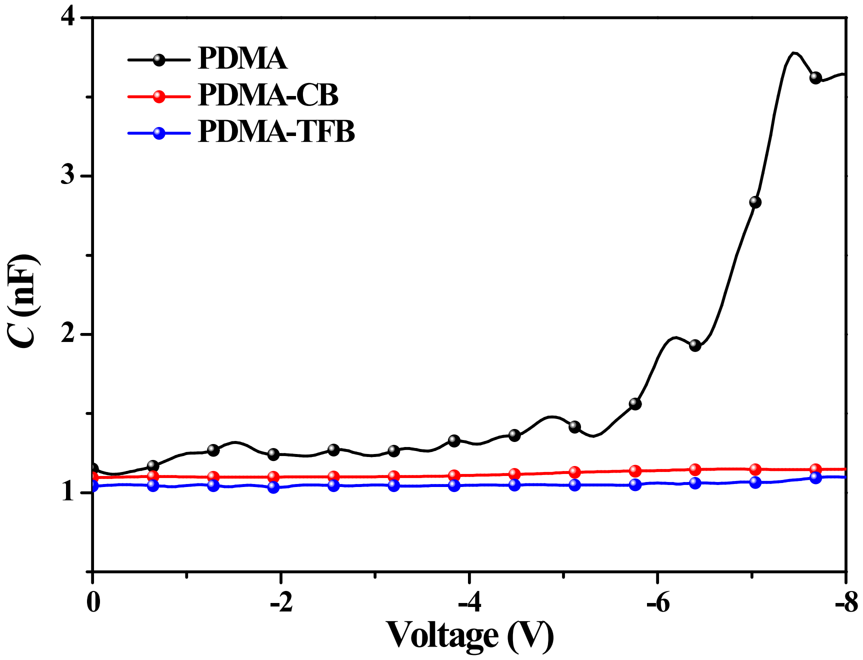

Figure S6. The *C*-*V* measurements of the PDMA, PDMA-CB, and PDMA-TFB perovskite devices (ITO/ZnO/PEIE/perovskite/TFB/MoO_3/Au). The values of *C* can be determined to the saturated part towards the negative voltage in the *C*-*V* curves. The equation of $\varepsilon = (CL)/(\varepsilon_0 S)$ can be used to calculate the ε, where ε_0, L and S represent vacuum permittivity, the thickness of the perovskite film and device area, respectively.

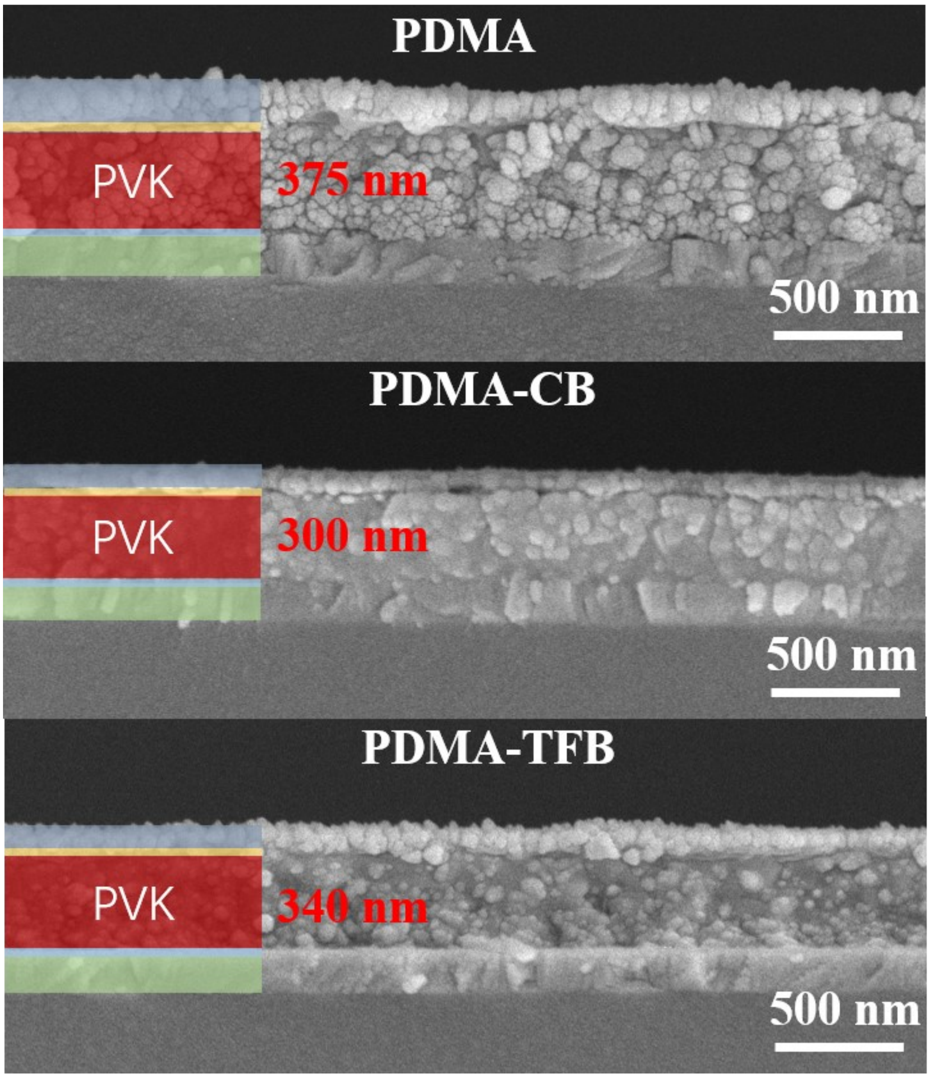

Figure S7. The cross-section scanning electron microscopy (SEM) of PDMA, PDMA-CB, and PDMA-TFB perovskites based on the device structure of indium tin oxide (ITO) (green)/ZnO-polyethylenimine ethoxylated (PEIE) (blue)/perovskite (red)/poly-[(9,9-dioctylfluorenyl-2,7-diyl)-alt-(4,4′-(*N*-(4-butylphenyl) (TFB) (yellow)/MoO_3-Ag (purple).

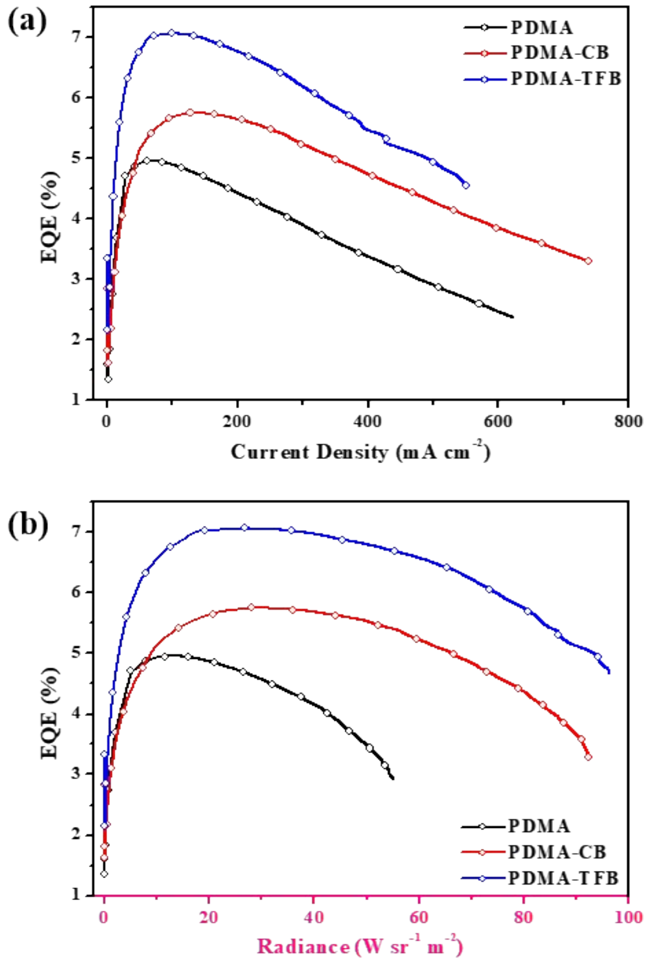

Figure S8. (a) EQE-current density curve and (b) Radiance-dependent EQE of various treatment PeLEDs.

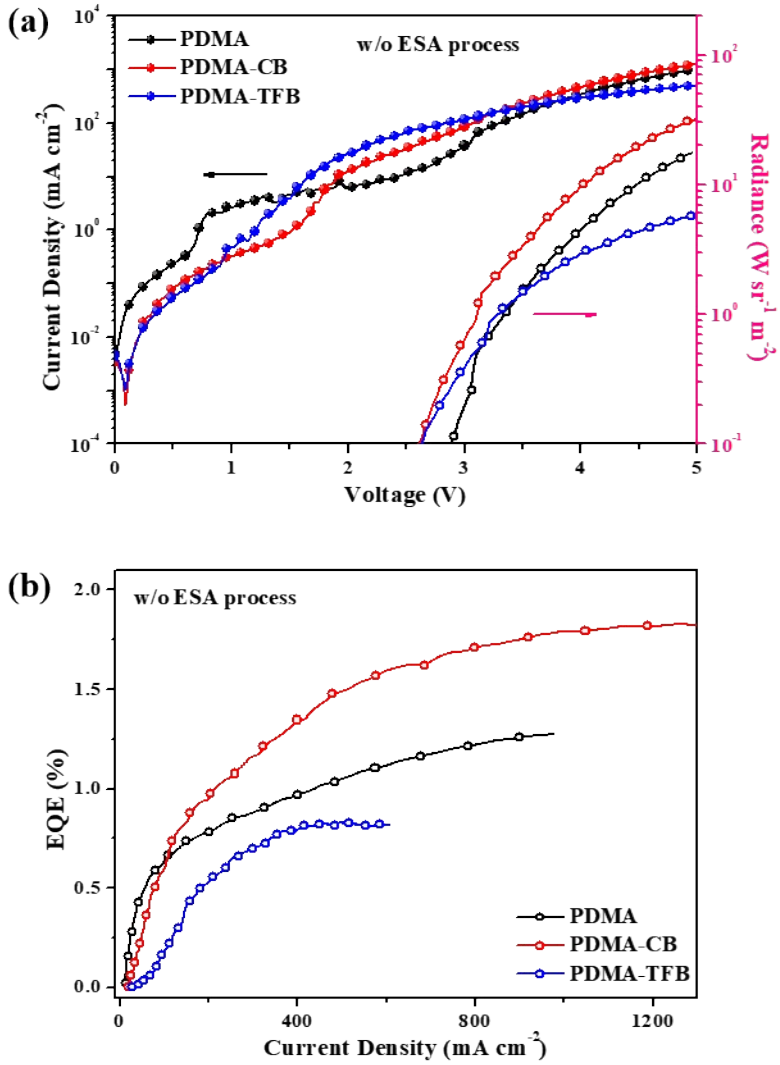

Figure S9. Characteristics of q-2D type PeLEDs without ESA process. (a) Current density-voltage-radiance curves. (b) EQE-current density curve.

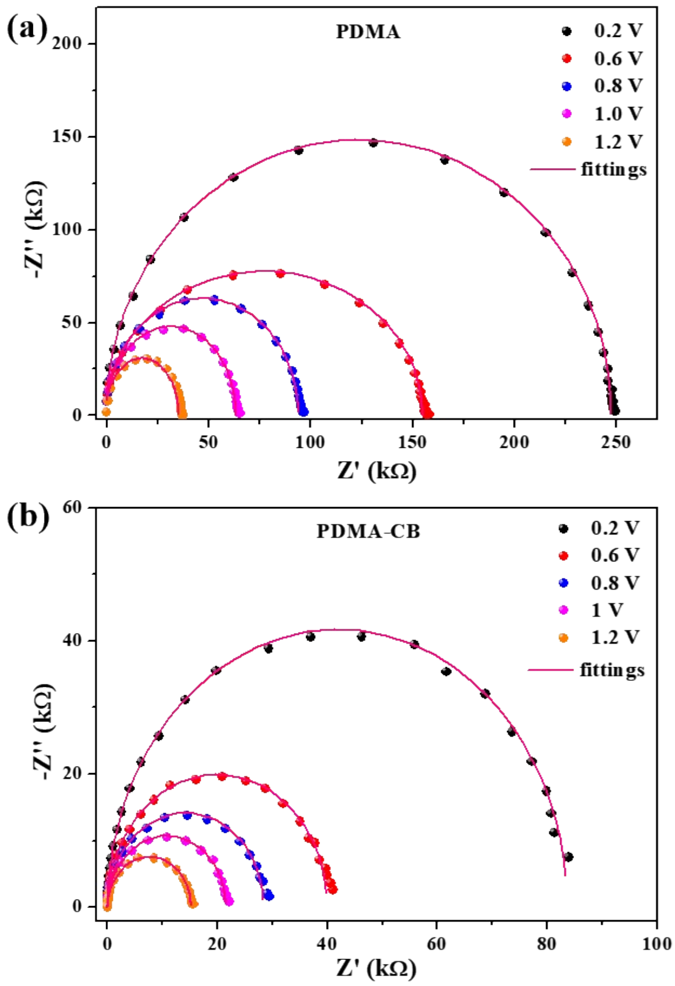

Figure S10. Nyquist impedance spectra for the PDMA (a) and PDMA-CB (b) PeLED devices.

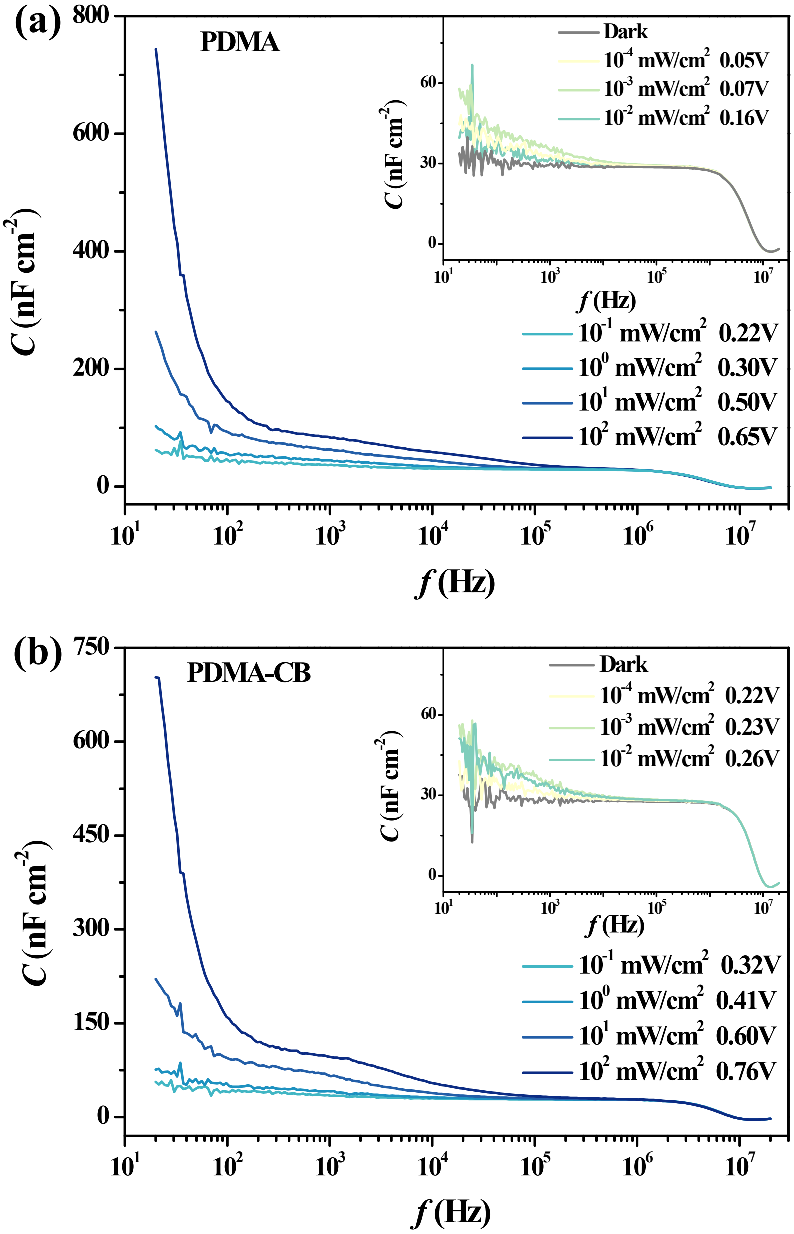

Figure S11. Room temperature *C-f* spectra for (a) the PDMA and (b) PDMA-CB PeLEDs measured at different light intensity with the bias voltage corresponding to the light-induced built-in voltage.

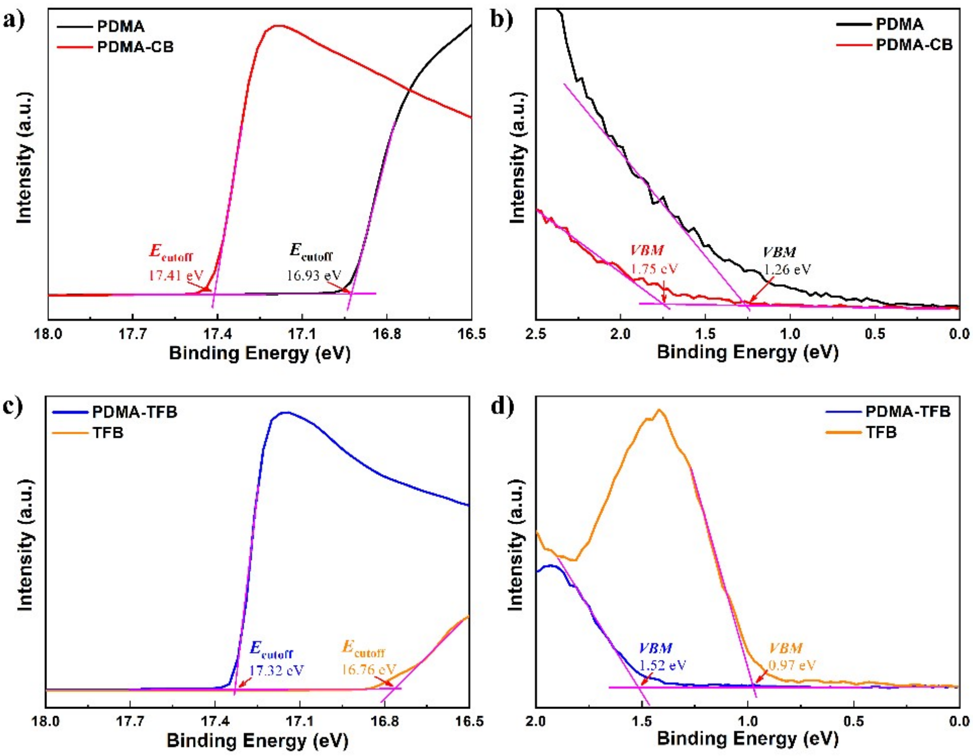

Figure S12. UPS spectra of different films on ITO/ZnO/PEIE substrates. (a)(c) photoemission cutoff (E_{cutoff}) and (b)(d) valance-band region (E_F).

The related values to extract UPS data have been shown in the Figure S8. The value of E_{cutoff} are 16.93 eV (PDMA), 17.41 eV (PDMA-CB), 17.32 eV (PDMA-TFB) and 16.76 eV (TFB), respectively. The value of E_F are 1.26 eV (PDMA), 1.75 eV (PDMA-CB), 1.52 eV (PDMA-TFB) and 0.97 eV (TFB). The valance-band of PDMA, PDMA-CB, PDMA-TFB, and TFB films are calculated to be **-5.53 eV, -5.52 eV, -5.41 eV and -5.40** eV, respectively.

Table S2. Summary of FWHM of quasi-2D perovskite XRD profiles with various treatments.

	(002) (2θ°)	**(111) (2θ°)**
PDMA	0.35	0.60
PDMA-CB	0.34	0.63
PDMA-TFB	0.31	0.54

Table S3. The summary of quasi-2D PeLED performance without the ESA process.

	V_T (V)	**EQE (%)**	**J (mA cm^{-2})**	**R (W sr^{-1} m^{-2})**
PDMA	2.9	1.3	975	18
PDMA-CB	2.6	1.8	1076	34
PDMA-TFB	2.6	0.8	495	7

Table S4. Fitting parameters were obtained from time-resolved photoluminescence decay transients and the quantum yields (PLQY) of quasi-2D perovskite films with various treatments.

	τ_1 (ns)	**A_1**	**τ_2 (ns)**	**A_2**	**τ_{avg} (ns)**	**PLQY(%)**
PDMA	12	0.69	144	0.31	53	69
PDMA-CB	14	0.63	155	0.37	66	93
PDMA-TFB	16	0.70	150	0.30	56	81

Table S5. The parameters are obtained by fitting from the impedance spectra.

PDMA	**R_s (Ω)**	**R_{ct} (kΩ)**	***C* (nF)**
0.2 V	71	297	1.129
0.6 V	70	156	1.145
0.8 V	69	127	1.161
1.0 V	65	96	1.215
1.2 V	61	62	1.346

PDMA-CB	**R_s (Ω)**	**R_{ct} (kΩ)**	***C* (nF)**
0.2 V	40	83	1.089
0.6 V	40	39	1.095
0.8 V	40	28	1.101
1.0 V	40	21	1.105
1.2 V	39	15	1.096

PDMA-TFB	**R_s (Ω)**	**R_{ct} (kΩ)**	***C* (nF)**
0.2 V	45	174	1.107
0.6 V	45	61	1.105
0.8 V	45	50	1.109
1.0 V	45	29	1.109
1.2 V	45	3	1.100